Journal of Organometallic Chemistry 903 (2019) 120985

Contents lists available at ScienceDirect

Journal of Organometallic Chemistry

journal homepage: www.elsevier.com/locate/jorganchem

# Sustainable dipolar homo-dicopper (II) dihydrazone complex as a catalyst for Sonogashira cross couplings

Mohamed Shaker S. Adam [a, b]

[a] Department of Chemistry, College of Science, King Faisal University, P.O. Box 380 Al Hofuf, 31982, Al Ahasa, Saudi Arabia
[b] Chemistry Department, Faculty of Science, Sohag University, Sohag, 82534, Egypt

ARTICLE INFO

*Article history:*
Received 7 June 2019
Received in revised form
23 August 2019
Accepted 15 October 2019
Available online 21 October 2019

*Keywords:*
Salicylidene succinyldihydrazone
Copper (II)
Sonogashira cross-couplings
Homogeneous catalysis
Ionic liquids

ABSTRACT

A novel dicopper (II) complex, $Cu_2L$, was prepared form the complexation of the new polydentate ligand ($H_4L$), *bis*(sodium 3-formyl-4-hydroxybenzenesulfonate)succinylhydrazone, with copper acetate. The novel homobinuclear complex was quite characterized by various physico-chemical tools and employed as a homogeneous and efficient-green catalyst for Sonogashira cross-couplings of phenylacetylene with halobenzenes under sustainable conditions. $Cu_2L$ exhibited very good catalytic performance with excellent chemoselectivity. The catalytic efficiency of $Cu_2L$ was improved by using ionic liquids–aqueous media (1: 1, binary mixture). A mechanistic pathway was also proposed for Cu(II)-catalyzed Sonogashira cross-coupling reactions for the reported finding. DFT for $H_4L$ and $Cu_2L$ were studied. Electronic configurations, energy of HOMO and LUMO orbitals, energy gap between orbitals (ΔE), electronegativity, hardness and softness were also calculated and compared with the applicable catalytic findings of $Cu_2L$, which are in good conformity.



## 1. Introduction

Sonogashira cross-coupling is considering an imperative modern and powerful synthetic route for building up organic molecules mainly from alkynes, *i.e.* terminal acetylenes, with aryl, heteroaryl or vinyl halides. Such catalytic systems could take place within stoichiometric amounts of transition metal complexes, as catalysts, homogeneously or heterogeneously [1]. The wide applicability and diversity of Sonogashira C–C cross-couplings could be challenged in the synthesis of various organic materials, *e.g.* natural products, molecular materials, agrochemicals, non-linear optical materials, biologically active molecules, molecular electronics, acetylene macrocycles, dendrimer and polymeric materials [1,2]. The most catalytic methodologies were developed mainly for Pd(II)-complexes catalysts [3–8]. Likewise, copper-mediated development of Sonogashira coupling protocols instead of Pd-catalyzed homogeneously or heterogeneously [6], as Pd-free systems, due to its less toxicity and economically cost-effective [9,10]. Hence, those findings highlighted the role of copper (I)/(II) ion and its tolerated pincer chelated ligands, *e.g. N*-heterocyclic carbenes [11], phosphoryl-phenanthrolines [12], phosphine-ferrocenes [13] and oxaloyldihydrazone [14], to improve the Sonogashira coupling catalytic processes.

The strong coordination capability of the symmetrical dihydrazones towards *nd* metal ion of the various oxidation states to form highly stable monometallic [15], heterobimetallic [16] and homo-bimetallic [17] complexes with alternative mode of bonding and stereochemistry [14,18], is considerable of interest. In particular, the elevated catalytic potential of the homobimetallic complexes, *e.g.* $MoO_2^{2+}$-complexes in various organic syntheses was reported lately and gave high catalytic sufficiency [19]. The catalytic reactivity of the homobinuclear Schiff base complexes of transition metal ions is observable higher than that of the mononuclear Schiff base complexes. This could be related to the synergic effect of two central metal ions in the complex catalyst framework [10,20].

In Sonogashira cross-coupling chemistry there is always detecting a side product, which mainly caused by the Glaser-type oxidative dimerization of the substrate, *i.e.* alkyenes. This undesirable side product is always a serious concern on large scale synthesis [21]. Moreover, the higher cost, toxicity, difficult handling of air and moisture sensitive coordinated *P,N*-ligands, longer reaction times, low yields and the environmentally unfriendly reaction conditions (*e.g.* applying of toxic amines as organic solvents or as bases [22]) are the motivation here to design a novel and economically cost-effective sustainable polar homobinuclear

*E-mail addresses:* madam@kfu.edu.sa, shakeradam61@yahoo.com.

https://doi.org/10.1016/j.jorganchem.2019.120985
0022-328X/

copper (II)-dihydrazone complex as an effective homogeneous catalyst for Sonogashira cross-couplings under various sustainable conditions.

## 2. Experimental

### 2.1. Reagents and apparatus

Chemicals and reagents were purchased from Merck and Sigma-Aldrich. All were used in chemical reactions without any treatment. With a GMBH VarioEl model V2.3 apparatus, the percentages of carbon, hydrogen and nitrogen atoms in their compounds were analyzed and determined. NMR spectral scans were predicted with a machine Bruker ARX400 multinuclear NMR spectrometer at 400.1 MHz for $^{1}$H-nuclei and at 100.6 MHz for $^{13}$C-nuclei at 25 °C. Chemical shift magnitudes ($\delta$ in ppm) of $^{1}$H and $^{13}$C nuclei and their corresponded coupling constants for H nuclei ($J_{HH}$) were evaluated for the ligand ($H_4L$). The electronic transition spectra were achieved for the studied ligand ant its corresponding Cu-complex in the given solvent (water) using the JASCO machine as UV–Vis. spectrophotometer (model V-570) with a 10 mm silica cells in a thermostatted cell holder. Fourier Transform Infrared spectrophotometer Shimadzu FTIR-8101 was applied to measure the stretching vibrational bands in the region from 4000 to 400 cm$^{-1}$. Thermogravimetric analysis was studied for $H_4L$ and $Cu_2L$ using Shimadzu TGA-50H thermal analyzer with flow rate of nitrogen gas, as an inert carrier gas, 20 cm$^3$ min$^{-1}$ and with heating rate, from 30 to 400 °C, 10 °C min$^{-1}$. Mass spectroscopy of $H_4L$ and $Cu_2L$ was appreciated by waters Qtof Micro YA263 mass spectrometer in $m/z$. Conductivity of $H_4L$ and $Cu_2L$ in various media was determined by a Jenway conductometer of 4320 model supplied by an epoxy bodied conductivity cell (consisting of two electrodes, shiny) at 25 °C in water bath using a HAAKE model F3-k ultra-thermostat with cell constant calibration at 0.01–19.99. Magnetic measurements for $Cu_2L$ were achieved by Gouy's balance with Pascal's contents using $Hg[Co(SCN)_4]$ for diamagnetic correction calibration. Metrohm 695 pH/ion meter to ±0.005 units were used to determine the pH at 25 °C. Estimation of the melting point was taken place by a Thermo Scientific 9100 machine.

### 2.2. $H_4L$ preparation

With modification of benzene-1,4-dicarbohydrazide condensation with aldehydes or ketones [19,23], in 50 mL $H_2O$, 4.48 g (20.0 mmol) of sodium 3-formyl-4-hydroxybenzenesulfonate was mixed leisurely with 50 mL of an aqueous solution of 1.46 g (10.0 mmol) of succinyldihydrazide and refluxed for 3 h with continuous stirring at 100 °C. The completion of the reaction was monitored by TLC within the formation of pale yellow color in the solution. Water was removed after completion of reaction by slow evaporation in vacuum. The solid material was collected and washed with cooled ethanol, and then dried in oven. It was enough pure by NMR to be used in the next step without any additional purification. The product was isolated as pale yellow color solid with 89% yield.

$^{1}$H NMR of diketone form ($H_4L$) (DMSO-$d_6$, 400 MHz): $\delta$ 3.36 (s, $CH_2$, 4H), 7.39 (s, 2H), 7.81–7.94 (m, 4H), 8.59 (s, 2H), 11.51 (s, 2H, −CH═N—) and 11.68 ppm (s, 2H, NH). The characteristic $^{1}$H NMR of the tautomeric forms (dienole and keto-enole): 2.58 (t, $^{3}J = 6.8$ Hz), 8.05 (s) and 8.19 ppm (s).

$^{13}$C NMR (100 MHz, DMSO-$d_6$, dept-135): $\delta$ 27.00 ($CH_2$), 119.90 (CH), 124.25 (CH), 137.25 ($C_q$), 143.52 (CH), 146.33 ($C_q$), 149.92 (CH), 153.60 ($C_q$), 168.54 (CH, CH═N) and 174.24 ppm ($C_q$, C═O). ($^{1}$H-, $^{13}$C NMR and dept-135 spectra are presented in Figs. S1–S3, the supplementary materials). The characteristic $^{1}$H NMR of the tautomeric forms (dienole and keto-enole form): 27.66, 28.95, 29.49 ($CH_2$). $^{13}$CNMR: 119.97, 120.18 (CH), 124.69 (CH), 137.29 ($C_q$), 143.70 (CH), 146.51 ($C_q$), 153.64, 153.74, 153.80 ($C_q$), 168.79 (CH, −CH═N—) and 174.05 ppm ($C_q$, C═O).

IR spectra (wave number, $\bar{\nu}$, cm$^{-1}$): 3399 (O—$H_{phenolic}$), 3213 (N—H), 2983 (C—$H_{alphatic}$, $-C_2H_4$), 1679 (C=$O_{keto}$), 1284 (C—O), 1647 and 1616 (C=$N_{azomethine}$), 1550 (NH—CO), 1158 (C—$N_{azomethine}$), 1480 (S═O) and 1145 cm$^{-1}$ (S—O$^-$).

### 2.3. Copper complexes preparation [$\mu^2$-$N_2$,$N_2$'-bis(sodium 3-formyl-4-oxidobenzylidenesulfonate)benzene-1,3-dicarbohydrazidato]-bis [aquacopper (II)] monohydrate ($Cu_2L$)

In an aqueous media (50 mL) of $H_4L$ (2.79 g, 5.0 mmol) was gently poured to an aqueous solution of copper acetate monohydrate, $Cu(OAc)_2.H_2O$ (1.99 g, 10.0 mmol, 50 mL) at room temperature. The resulted mixture was heated up to 80 °C with continuous stirring for 3 h with gradual turning of the solution color from pale yellow to green. The reaction mixture was cold down to room temperature, the solvent was evacuated and the residual was collected and washed by cooled ethanol and dried in oven for 4 h. Recrystallization of the complex was carried out in a 1:1 mixture of $H_2O$ (30 mL) and ethanol (30 mL). The pure product was isolated as green color solid with 69% yield.

IR spectra (wave number, $\bar{\nu}$, cm$^{-1}$): 3392 and 1653 (O—$H_{water}$), 3065 (C—$H_{aromatic}$), 2997 (C—$H_{alphatic}$, $-C_2H_4$), 1288 (C—O), 1603 and 1568 (C=$N_{azomethine}$), 1525 (NH—CO), 1158 (C—$N_{azomethine}$), 1456 (N═C—O$^-$), 1375 (S═O), 1135 cm$^{-1}$ (S—O$^-$), 883 (Cu—O) and 592 cm$^{-1}$ (Cu—N).

### 2.4. Catalytic potential of $Cu_2L$

Sonogashira C–C cross-coupling reactions were carried out in two necked round flask connected with water circulation condenser charged with halobenzene derivatives (1.0 mmol) in 10 mL ethanol or given solvent (as shown below) in the presence of $Cu_2L$ as a homogeneous catalyst (0.02 mmol) and potassium carbonate or other bases (3.0 mmol). The reaction was initiated by addition of phenylacetylene (1.2 mmol) under reflux conditions at 80 °C for 24 h in a thermostated oil bath under $N_2$ atmosphere. The reaction mixture was cooled down to room temperature. The crude products were extracted by filtration because the products are quite insoluble in the reaction mixture (in aqueous and in aqueous-ionic liquid mixtures), especially after cooling down to room temperature. The yield amounts of the target products were evaluated by dissolving the crude product diethyl ether (10 mL) and by drawing a sample potion (0.1 mL) and submitted to the GC-MS. Purification of the final carried out by column chromatography using silica gel (by n-hexane 80%: ethyl acetate 20%).

The biarylethyne products were confirmed by $^{1}$H- and $^{13}$C NMR spectra (Figs. S4–S10, supplementary materials) and their yield percentages were determined with Shimadzu Gas Chromatography mass spectrometer (GC-MS) model QP2010 SE, with Rxi-5 Sil MS capillary column (30 m length × 0.25 mm ID × 025 μm film thickness). Injecting processes were taken place within auto-injection to the GC-MS at room temperature. The oven temperature of GC was started at 40 °C and fixed for 60 s, and then followed by a rate increase of temperature with 10 °C per min up to 200 °C. The inlet mode carried out with splitless at 200 °C. The carrier gas was high pure Helium gas with purity at 99.999% with flow rate 1 mL per min. Lab solution software of the connected PC was used in order to determine the yield percentages of the target products depending upon MS results.

### 2.5. Reusability of $Cu_2L$

The recycling of $Cu_2L$ was tested by repeating of Sonogashira cross-coupling reaction of phenylacetylene (1.0 mmol) with bromobenzene (1.0 mmol) in 10 mL of [bmim][$PF_6$]: $H_2O$ (1: 1) mixture at 80 °C for 20 h. The final product was easily extracted from the reaction media in the aqueous-ionic liquid by filtration due to its insolubility. Again, the reusability of $Cu_2L$ was probed by adding new amounts of the reactants in the same reaction media for several runs. The final product was determined by GC-MS analyses.

### 2.6. Computational treatments

Gaussian 09 revision c.01 [24] was applied for the computational data of DFT for $H_4L$ and $Cu_2L$. The geometrical molecular structures of $H_4L$ and $Cu_2L$ were optimized and given in the gas and in water phases within B3LYP and 6−31g(d,p) for carbon, hydrogen, oxygen, nitrogen, sodium and sulfur atoms. For $Cu^{2+}$ ions, the stochastic dislocation dynamics (SDD) basis set with effective core potential was motivated. Concerning the model of conductor-like polarizable continuum (CPCM) and the optimal geometrical structures in the water phase were accomplished at the B3LYP level. The values of frontier molecular orbitals according to Koopman theorem were associated with ionization potential ($I$) and electron affinity ($A$) and evaluated from Eqs. (1) and (2)) [25].

$$I = -E_{HOMO} \quad (1)$$

$$A = -E_{LUMO} \quad (2)$$

Consequently, the electronegativity, χ, global harness, η, softness, σ, and electrophilicity index (ω) could be derived calculatingly for $H_4L$ and $Cu_2L$ from Eqs. (3)–(6) [25].

$$\chi = \frac{1}{2}(I + A) \quad (3)$$

$$\eta = \frac{1}{2}(I - A) \quad (4)$$

$$\sigma = \frac{1}{\eta} \quad (5)$$

$$\omega = \chi^2 / 2\eta \quad (6)$$

## 3. Results and discussion

### 3.1. Synthesis and characterization

Succinyldihydrazide was synthesized previously [19,23], which involved preparing the novel dipolar polydentate ligand ($H_4L$). $H_4L$ was synthesized by direct condensation of 1 equivalent of succinyldihydrazide with 2 equivalents of sodium 3-formyl-4-hydroxybenzenesulfonate [26] in water, without any external motivation, *e.g.* a catalyst. $^1$H- and $^{13}$C NMR, IR, UV−Visible and mass spectra, EA (elemental analyses), and conductivity measurements were carried for the molecular structural conformation of $H_4L$ (Table 1).

Significantly, $^1$H-, $^{13}$C NMR and dept-135 spectral scans of $H_4L$ are presented in Figs. S1−S3 in the supplementary materials. At 3.36 ppm, a singlet resonating signal of the succinyl —$C_2H_4$— protons was assigned. Two high shift singlet signals were displayed at 11.51 and 11.68 ppm are corresponded to azo-methine (—CH═N—) and amino (>NH) groups, respectively, due to the intramolecular hydrogen bonding [15−17].

$^{13}$C NMR spectra show distinguished signals for —$C_2H_4$— group and the azo-methine group (—CH═N—) at 27.00 and 174.05 ppm, respectively. Particularly, the tautomerism of such aroyl salicylidene dihydrazones has been elucidated previously [18,23], as diketone, keto-enol, and dienol tautomers. The tautomerism of $H_4L$ could be detected by $^1$H- and $^{13}$C NMR spectra. Singlet signals at 2.56, 2.58 and 2.60 ppm of hydrogen protons demonstrated the tautomerism for the succinyl-$C_2H_4$ group. Also, $^{13}$C NMR manifested some additional signals referring to tautomeric structures at 168.79 ppm for the azo-methine and 174.05 ppm amido group (>C═O). Moreover, the succinyl-$C_2H_4$ group assigned some additional signals in the aliphatic region at 27.66, 28.95 and 29.49 ppm [23].

Copper acetate monohydrate reacted with $H_4L$ to form a novel homo-dicopper pincer chelate complex ($Cu_2L$) in an aqueous media within 2: 1 equivalents of $Cu^{2+}$: $H_4L$, respectively, with good yield (Table 1), similar to the previously reported syntheses [30−33]. Alternative technical tools were applied to elucidate the tentative molecular geometry of the novel Cu-complex (Table 1).

In the solid phase, both $H_4L$ and $Cu_2L$ exhibited high air stability with decomposed temperature at 264 and > 300 °C, respectively (Table 1). The wide range of pH stability from 1.9 to 9.4 was determined for $H_4L$ and $Cu_2L$ aqueous solutions in the standard universal buffers [19]. The stoichiometric molar ratios of $Cu^{2+}$ and $H_4L$ solutions were estimated spectrophotometrically by continuous variation method (Fig. S11). The carbon, hydrogen and nitrogen percentages of the elemental analyses for $H_4L$ and $Cu_2L$ seem to be in accordance with the theoretical percentages for the proposed structure with small difference ±0.4%, referring to the high purity (Table 1).

$H_4L$ and $Cu_2L$ exhibited strong solubility in water and in solvents with high coordination power, dimethylsulfoxide (DMSO) *N,N′*-dimethylformamide (DMF). Both ligand and Cu-complex are sparingly soluble in acetonitrile and ethanol. Due to the very low solubility of benzene-1,4-dicarbohydrazides, *e.g.* succinyldihydrazone [19,27−29], the substituted sodium sulfonate group ($Na^+$ $SO_3^-$—) enhanced their solubility. Hence, the molar conductivities ($\Lambda_m$) of $H_4L$ and $Cu_2L$ were evaluated in DMSO, DMF, and water, as shown in Table 1. The conductivity results present three counter ions in solution per molecule, two of them are sodium ions and one is the complex anion as disulfonate anion $-SO_3^-$. The magnetic susceptibility of $Cu_2L$ was measured to afford *para*-magnetic character with magnetic values 6.21 B M. Magnetic properties of $Cu_2L$ could assign that no metal-metal ions interaction [34], as remarked elsewhere [31,33].

The electronic spectra of aqueous solutions of $H_4L$ and $Cu_2L$ showed the possible considerable electronic transitions, which displayed in Fig. 1 and listed in Table 1. At the UV-region, $H_4L$ exhibited three high-energy electronic transitions bands of $\pi \rightarrow \pi^*$ at 240 nm and of $n \rightarrow \pi^*$ at 288 and 294 nm. An additional band in the low energy visible region was assigned for the ligand charge transfer at 325 nm [35]. All electronic transitions bands were influenced by the ligand's coordination to $Cu^{2+}$ ions. Both bands for $\pi \rightarrow \pi^*$ and of $n \rightarrow \pi^*$ were little shifted to lower energy at 248, 277 and 315 nm, respectively. Particularly, the ligand CT band was disappeared and a new lower energy band was assigned at 372 nm, resulted from the ML-CT transition (Table 1) [17]. A very broad absorption band was found at 436 nm for the $d \rightarrow d$ transition of the metal ion ($^2Eg \rightarrow {}^2T_2g$).

The significant IR spectral absorption signals of $H_4L$ and $Cu_2L$ are shown in Figs. S12 and S13 in the supplementary materials. The assigned diagnostic signals of OH—phenolic and NH—amido

**Table 1**
CHN analyses, melting point, electronic spectral transitions of $H_4L$ and $Cu_2L$ at concentration $1.0 \times 10^{-5}$ mol dm$^{-3}$ in water at 25 °C and molar conductivities, $\Lambda_m$, of $H_4L$ and $Cu_2L$ with concentration at $1.0 \times 10^{-3}$ mol dm$^{-3}$ in $H_2O$, DMF and DMSO at 25 °C.

| Comp. | MW (g mol$^{-1}$) | Color | CHN analysis found %, (calc. %) | | | m.p. (°C) | UV–Vis. spectra | | | $\Lambda_m$ ($\Omega^{-1}$ cm$^2$ mol$^{-1}$) | | |
|---|---|---|---|---|---|---|---|---|---|---|---|---|
| | | | C | H | N | | $\lambda_{max}$ (nm) | $\varepsilon$ (mol$^{-1}$cm$^{-1}$) | Assign. | $H_2O$ | DMF | DMSO |
| $H_4L$ | 558.44 | Pale yellow | 39.03 (38.71) | 2.71 (2.89) | 9.84 (10.03) | 264 decom. | 325 | 6451 | LCT n→π* | 363 | 232 | 209 |
| | | | | | | | 294 | 8112 | n→π* | | | |
| | | | | | | | 288 | 8236 | π→π* | | | |
| | | | | | | | 240 | 10451 | | | | |
| $Cu_2L$ | 735.55 | Green | 29.10 (29.39) | 2.26 (2.47) | 7.75 (7.62) | >300 | 436 vbr | 5132 | d-d | 401 | 218 | 188 |
| | | | | | | | 372 br | 7691 | ML-CT n→π* | | | |
| | | | | | | | 315 | 8879 | n→π* | | | |
| | | | | | | | 291 | 8911 | π→π* | | | |
| | | | | | | | 277 | 12753 | π→π* | | | |
| | | | | | | | 248 | 12805 | | | | |

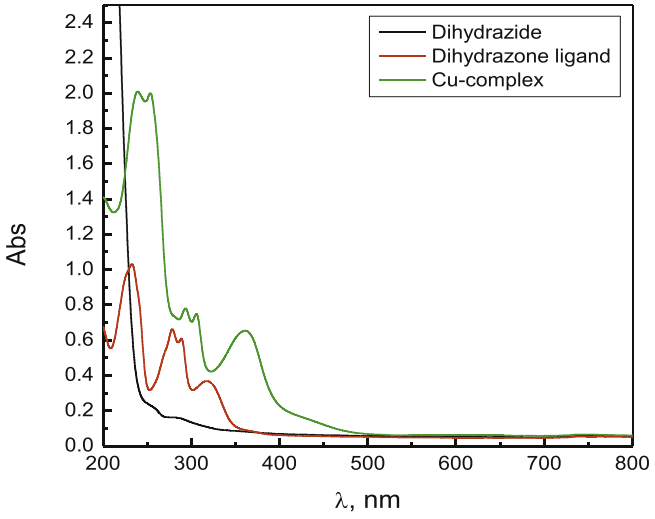


**Fig. 1.** UV/Vis. spectral scans of dihydrazone ligand ($H_4L$) and Cu-complex ($Cu_2L$) with concentration of the compounds [Compound] = $1.0 \times 10^{-5}$ mol dm$^{-3}$ at 25 °C in water.

moieties in $H_4L$ at 3399 and 3213 cm$^{-1}$ were disappeared due to the coordination of the dienolized $H_4L$ to $Cu^{2+}$ ions. This behavior could be elucidated also by the striking disappearance of the characteristic C=O vibrational signal at 1679 cm$^{-1}$ of $H_4L$ after complexation with $Cu^{2+}$ ions. Furthermore, the obvious absorption band shift of the azo-methine group in $H_4L$ from 1647 to 1616 cm$^{-1}$ to 1603 and 1568 cm$^{-1}$, respectively, is caused by the bounding of nitrogen with its lone pair of —C=N— group to the central metal ion [28,29]. Solvent molecules, *i.e.* water, as liable coordinated molecules or a crystalline molecule could be also detected by the presence of new stretching vibrational bands at 3392 and 1653 cm$^{-1}$ in $Cu_2L$ [25,26]. The notable vibrational spectral bands at 1145 and 1480 cm$^{-1}$ of the recognized sulfonate S–O$^-$ and S=O stretching bonds, respectively, were influenced by the complex formation with $Cu^{2+}$ ions to be at 1135 and 1375 cm$^{-1}$, respectively [25,26]. Moreover, there are two supplemental weak absorption bands of the formed M—O, and M—N bonds in $Cu_2L$ were displayed at 883 and 592 cm$^{-1}$, respectively [19,26].

Mass spectroscopic results for $H_4L$ and $Cu_2L$ are shown in Figs. S14 and S15 in the supplementary materials, respectively. $H_4L$ has mass peak at 582.4 m/z for [M + Na$^+$] and at 559.2 m/z for [M + 1]. Mass spectra of $Cu_2L$ show base peaks for the molecular structure as [M + Na$^+$] at 740.57 m/z and as [M + 1] at 718.33 m/z (Scheme 2). Other characteristic mass peaks for $Cu_2L$ were detected at 831, 662, and 543 m/z.

Water molecules in the crystal lattice or in the coordination sphere, as labile coordinated solvent, in $Cu_2L$ were estimated by thermogravimetric analyses (TGA) (Fig. S16, supplementary materials). From TGA, there were found two decomposed successive steps. In the first step, the mass loss percentage was discovered in the range between 100 and 140 °C with mass lose percentage $\Delta m_{rel} = 2.2\%$, which almost agreed with the predictable value ($\Delta m_{cal.} = 2.5\%$). This decomposition step refers to the number of solvated crystalline water molecules (one molecule). In the second step, the mass lose percentage was remarked in the range of 185–230 °C, in which the derived mass lose was $\Delta m_{rel} = 4.6\%$, whereas, the expected mass loss percentage was calculated to be $\Delta m_{cal.} = 4.4\%$. The second mass loss is attributable to the loss of two labile water molecules in the coordinated sphere in $Cu_2L$ (Scheme 1) [26]. $H_4L$ did not show any observable decomposition steps for the temperature range up to 400 °C showing high thermal stability.

### 3.2. Catalytic processes

The catalytic feature of $Cu_2L$ was evaluated in Pd-free Sonogashira C–C reaction of phenylacetylene (1.2 mmol) with halobenzene (bromobenzene or iodobenzene, 1.0 mmol) in various reaction conditions, homogeneously, as a standard model for Sonogashira cross-coupling reactions. Fig. 2 shows the optimal required time for the highest yield of the chemoselective, which reported after 20 h affording 89% of 1,2-diphenyethyne at 80 °C in ethanol, as an environmentally friendly and reasonable cheap solvent, in the presence of $K_2CO_3$, (Table 2). Under various reaction conditions of solvents and bases in the optimal time, $Cu_2L$ mediated the catalytic reactions and the obtained yield percentages were listed in Table 2. The products were characterized in pure form by NMR spectra and their yield in percentages were determined by GC-MS.

To define the impact of the solvent, the reducing character of the coordinated *bis*-ONO ligand in $Cu_2L$ or the base, the reaction proceeded in ethanol provided good yield of the desired product (entry 1, 89%) by using $K_2CO_3$ as a base, whereas, with NaOAc, the yield was less than half (entry 2, 42%). By using more stronger base (Nat*B*uO), there was very little improvement in the yield of 1,2-diphenyethyne than that with NaOAc (entry 3, 57%) (TON and TOF values). Hence, the best base combination with ethanol was found to be $K_2CO_3$, offered suitable results for such catalytic processes, and this could be resulted from the low reactivity of $K_2CO_3$ to avoid the undesired side products [9]. The yield was significantly reduced by using ethanol-water system (1: 1) in the presence of $K_2CO_3$ or Nat*B*uO (entries 4 and 5, 78% and 52%, respectively) [36]. This phenomenon was highly remarked, when the catalytic processes took place in pure water (entries 6–8, with $K_2CO_3$, NaOAc or Nat*B*uO, respectively, as observed from TON and TOF values). Initiating the catalytic processes in water could probably reduce the

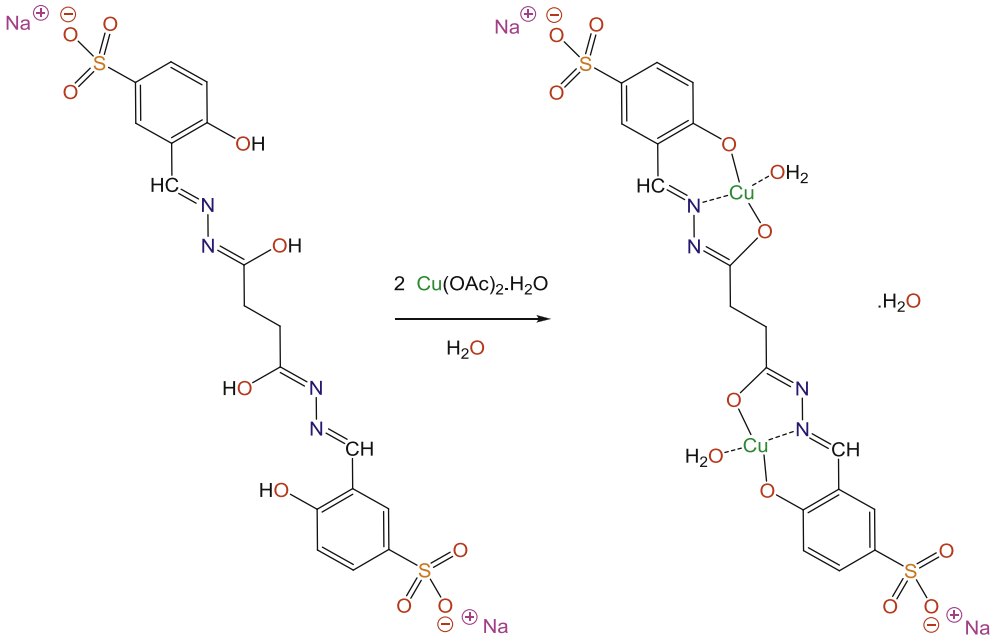


**Scheme 1.** Synthetic pathway of $Cu_2L$ form copper acetate monohydrate with $H_4L$ reaction.

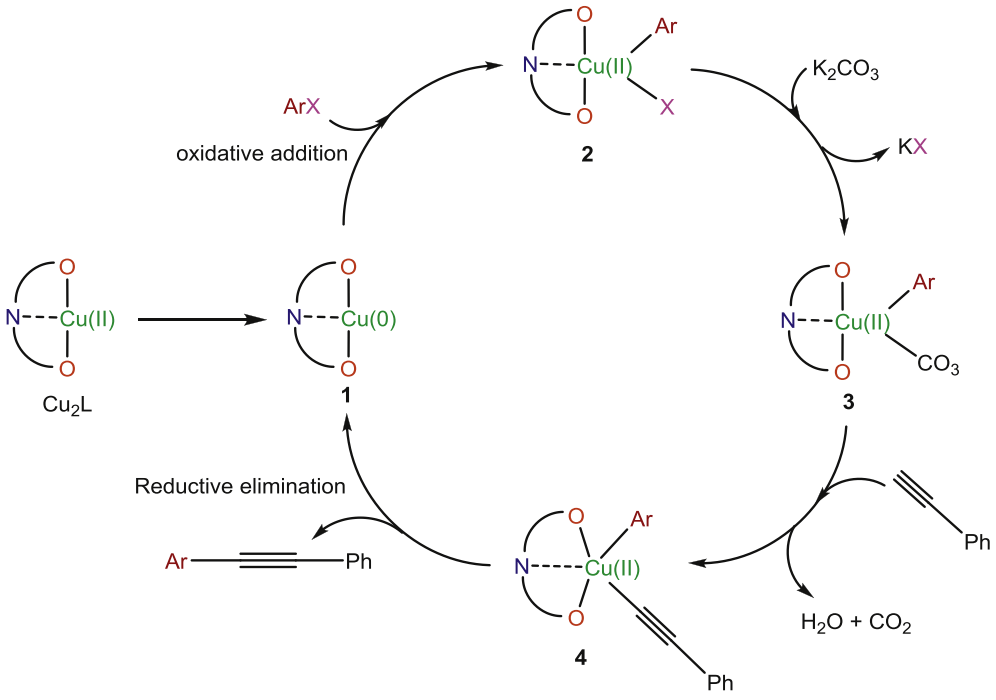


**Scheme 2.** Sonogashira cross-coupling reaction mechanism catalyzed by $Cu_2L$.

solubility and miscibility of the catalytic components [37,38]. Na*t*-BuO was little effective base than $Na_2CO_3$ in water, due to the immediate hydrolysis of Na*t*BuO to afford NaOH, as a strong base. Under free solvent system, the yield percentages of 1,2-diphenyethyne were moderate to good with $K_2CO_3$ or Na*t*BuO (entries 9 and 10, 77 and 54%, respectively). Indeed, the variation in polarity between the involved catalyst, as a high polar component, the substrates, phenylacetylene, and bromobenzene, as less polar components, could be the reason of less miscibility, as well as, it could reduce the reactivity of $Cu_2L$ towards the cross-coupling [9]. The catalytic processes under solvent-free conditions were found to be better than in water, Table 2. In high coordinated polar organic solvents, *i.e.* THF, DMF and DMSO, entries 11, 12 and 13, respectively, the reaction afforded low yield percentages of the chemoselective product. The strong coordination power of such solvents might be coordinated to $Cu^{2+}$ ion of the catalyst, and then capsulated the catalyst and considerably reduced its catalytic potential towards the cross-coupling [34]. Using acetonitrile, as a polar solvent, enhanced the progressing of the catalytic yield of 1,2-diphenyethyne, which could provide better solubility and

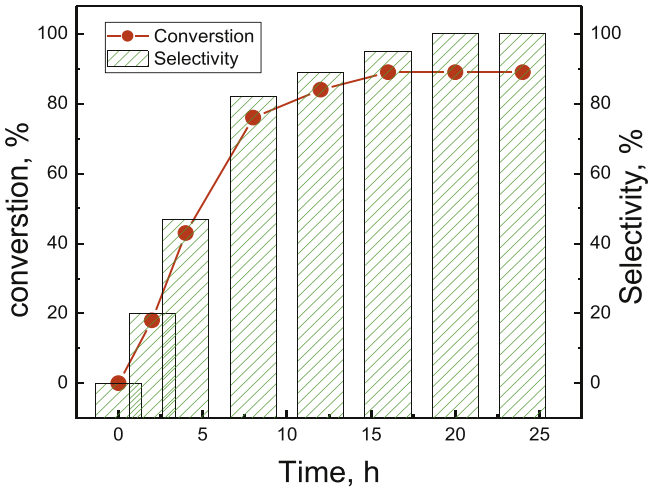


**Fig. 2.** The kinetic profile of the Sonogashira C–C coupling reaction of phenylacetylene and bromobenzene catalyzed by $Cu_2L$ in 10 mL of ethanol at 80 °C for 24 h.

miscibility to the catalyst and substrates similar to that in ethanol (entry 14, 85%). Glaser coupling product (homo-coupling) was formed as a major product (entry 15, 32%) when the reaction process was carried out under aerobic atmosphere, as observed elsewhere [39]. It could be deduced that the solvent in such catalytic processes plays a major role to enhance or to reduce the catalytic efficiency of the homogeneous $Cu_2L$ catalyst (this will be discussed in the mechanistic aspects).

The percentage load of the catalyst ($Cu_2L$) to the reaction showed a significant influence on the yield of the produced chemoselective product (Table 3). Without the catalyst, no significant amount of 1,2-diphenyethyne was detected (only ~10%, Table 3). The increased loaded catalyst to the reaction processes improved the yield percentages of the product, which was observed form 0.01, 0.02–0.05 mmol (81%, 89%, and 90%, respectively). However, when the catalyst loading was further increased to (0.10 mmol), it did not help to improve the yield percentages of the product but minor reduction was observed (88%) (as reported from TON and TOF values, Table 3).

**Table 3**
Effect of $Cu_2L$ loaded amount on Sonogashira C–C coupling reaction of phenylacetylene and bromobenzene.

| Entry[a] | Catalyst load (mmol) | Yield (%)[b] | TON[c] | TOF[d] |
|---|---|---|---|---|
| 1 | 0.00 | 10 | 0.0 | 0.00 |
| 2 | 0.01 | 81 | 81.0 | 4.05 |
| 3 | 0.02 | 89 | 44.5 | 2.22 |
| 4 | 0.05 | 90 | 18.0 | 0.90 |
| 5 | 0.10 | 88 | 8.8 | 0.44 |

[a] Phenylacetylene (1.2 mmol), bromobenzene (1.0 mmol) and base ($K_2CO_3$, 3.0 mmol) in 10 mL ethanol, at 80 °C for 20 h under $N_2$ atmosphere.
[b] The yield percentages of the C–C product analyzed by GC-MS.
[c] TON (turnover number) is the ratio of mmoles of product to mmoles of catalyst.
[d] The TOF (turnover frequency) (TON/h) is mmol (mmol catalyst)$^{-1}$ h$^{-1}$.

Comparatively, Beletskaya et *al.* [12] reported that the catalytic reactivity of Cu(I) diethoxyphosphoryl-phenanthroline complexes catalysts was recorded between 24 and 48 h for the C–C and C—heteroatom cross-couplings. Also, Tahsini et *al.* reported 24–48 h for the Sonogashira cross-coupling application to the optimized yield using Cu(II)–*N*-carbenes catalysts, homogeneously [11]. Moreover, dipalladium (II) ONO-pincer complex catalyzed copper-free Sonogashira coupling processes with optimal time 48 h in $H_2O$–DMSO mixture under homogeneous phase [36]. Chavan et *al.* reported the catalytic potential of heteroleptic Cu(I) complex of pyridyl-pyrazolone and triphenylphosphine in the cross-coupling of phenylacetylene with iodobenzene derivatives with consumed time about 16 h in presence of $K_2CO_3$ in toluene [9]. The internal formed complex between Cu(I) iodide and cyclohexane-1,2-

**Table 2**
$Cu_2L$ catalyzed Sonogashira C–C coupling reaction of phenylacetylene and bromobenzene in various solvents..

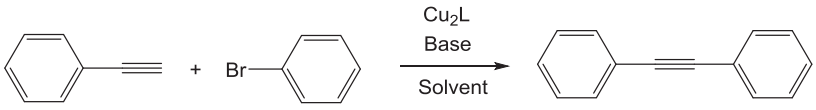


| Entry[a] | Solvent | Base | Yield (%)[b] | TON[e] | TOF[f] |
|---|---|---|---|---|---|
| 1 | Ethanol | $K_2CO_3$ | 89 | 44.5 | 2.22 |
| 2 | Ethanol | NaOAc | 42 | 21.0 | 1.05 |
| 3 | Ethanol | NatBuO | 57 | 28.5 | 1.42 |
| 4 | Ethanol:Water (1:1) | $K_2CO_3$ | 78 | 39.0 | 1.95 |
| 5 | Ethanol:Water (1:1) | NatBuO | 52 | 26.0 | 1.30 |
| 6 | Water | $K_2CO_3$ | 72 | 36.0 | 1.80 |
| 7 | Water | NaOAc | 68 | 34.0 | 1.70 |
| 8 | Water | NatBuO | 50 | 25.0 | 1.25 |
| 9 | Free solvent | $K_2CO_3$ | 77 | 38.5 | 1.92 |
| 10 | Free solvent | NatBuO | 54 | 27.0 | 1.35 |
| 11 | THF | $K_2CO_3$ | 53 | 26.5 | 1.32 |
| 12 | DMF | $K_2CO_3$ | 45 | 22.5 | 1.12 |
| 13 | DMSO | $K_2CO_3$ | 37 | 18.5 | 0.92 |
| 14 | AN | $K_2CO_3$ | 85 | 42.5 | 2.12 |
| 15[c] | Ethanol | $K_2CO_3$ | 32 | 16.0 | 0.80 |
| 16[d] | Ethanol | $K_2CO_3$ | 94 | 47.0 | 1.96 |

[a] Phenylacetylene (1.2 mmol), bromobenzene (1.0 mmol), base ($K_2CO_3$, 3.0 mmol), and $Cu_2L$ as a catalyst (0.02 mmol) in 10 mL solvent, at 80 °C for 20 h under $N_2$ atmosphere.
[b] The yield percentages of the C–C product analyzed by GC-MS.
[c] The reaction carried out under aerobic conditions.
[d] Copper acetate (0.02 mmol) was used as a homogeneous catalyst instead of $Cu_2L$ under the same conditions.
[e] TON (turnover number) is the ratio of mmoles of product to mmoles of catalyst.
[f] The TOF (turnover frequency) (TON/h) is mmol (mmol catalyst)$^{-1}$ h$^{-1}$.

**Table 4**
$Cu_2L$ catalyzed Sonogashira C–C coupling reaction of phenylacetylene and bromobenzene in aqueous-ionic liquid binary mixtures.

| Entry[a] | Ionic liquid | Yield (%)[b] | TON[g] | TOF[h] |
|---|---|---|---|---|
| 1 | [bmim][$Tf_2N$][c] | 58 | 29.0 | 1.45 |
| 2 | [bmim][$Tf_2N$]:$H_2O$ (3 : 1) | 67 | 33.5 | 1.67 |
| 3 | [bmim][$Tf_2N$]:$H_2O$ (1 : 1) | 70 | 35.0 | 1.75 |
| 4 | [emim][$Tf_2N$][d] | 52 | 26.0 | 1.30 |
| 5 | [emim][$Tf_2N$]:$H_2O$ (3 : 1) | 57 | 28.5 | 1.42 |
| 6 | [emim][$Tf_2N$]:$H_2O$ (1 : 1) | 66 | 33.0 | 1.65 |
| 7 | [omim][$Tf_2N$][e] | 48 | 24.0 | 1.20 |
| 8 | [omim][$Tf_2N$]:$H_2O$ (3 : 1) | 62 | 31.0 | 1.55 |
| 9 | [omim][$Tf_2N$]:$H_2O$ (1 : 1) | 72 | 36.0 | 1.80 |
| 10 | [bmim][$PF_6$][f] | 70 | 35.0 | 1.75 |
| 11 | [bmim][$PF_6$]:$H_2O$ (3 : 1) | 85 | 42.5 | 2.12 |
| 12 | [bmim][$PF_6$]:$H_2O$ (1 : 1) | 87 | 43.5 | 2.17 |

[a] Phenylacetylene (1.2 mmol), bromobenzene (1.0 mmol), base ($K_2CO_3$, 3.0 mmol), and $Cu_2L$ as a catalyst (0.02 mmol) in 10 mL desired solvent, at 80 °C for 20 h under $N_2$ atmosphere.
[b] The yield percentages of the C–C product analyzed by GC-MS.
[c] 1-Butyl-3-methylimidazolium bis(trifluoromethylsulfonyl)imide.
[d] 1-Ethyl-3-methylimidazolium bis(trifluoromethylsulfonyl)imide.
[e] 1-Octyl-3-methylimidazolium bis(trifluoromethylsulfonyl)imide.
[f] 1-Butyl-3-methylimidazolium hexafluorophosphate.
[g] TON (turnover number) is the ratio of mmoles of product to mmoles of catalyst.
[h] The TOF (turnover frequency) (TON/h) is mmol (mmol catalyst)$^{-1}$ h$^{-1}$.

diamine, as high effective homogeneous catalyst for Sonogashira C–C protocol of substituted terminal alkynes and halobenzenes, took 60 h at 130 °C with various reaction conditions [39]. Conclusively, $Cu_2L$ could be distinguished as a sufficient homogeneous catalyst for Sonogashira cross-couplings of phenylacetylene and halobenzenes in ethanol. The high catalytic efficiency of $Cu_2L$, like an eco-friendly catalyst, could resulted from the incorporated two central metal ion bonded to the ligand, *i.e.* the two central metal ions with synergic effect, as observed previously [12,14]. Additionally, the high reducing feature of the bonded ligand to $Cu^{2+}$ ion could progress such catalytic system by formation of the active catalyst intermediate (see the mechanism) [29], as well as, $K_2CO_3$ is considerable reactive base, as carboxylate salt [40].

To the best of our back knowledge, the influence of ionic liquids on Sonogashira cross-coupling protocols catalyzed by Cu(I)/(II) species was not enough reported, compared to Pd(II)-systems [41]. The influence of some ionic liquids with various ratios on the yield of the chemoselective product of phenylacetylene and bromobenzene cross-coupling was studied under the optimized reaction conditions and summarized in Table 4. 1-butyl-3-methylimidazolium *bis*(trifluoromethylsulfonyl)imide ([bmim][$Tf_2N$]), 1-ethyl-3-methylimidazolium *bis*(trifluoromethylsulfonyl) imide ([emim][$Tf_2N$]), 1-octyl-3-methylimidazolium *bis*(trifluoromethylsulfonyl)imide ([omim][$Tf_2N$]) or 1-butyl-3-methylimidazolium hexafluorophosphate ([bmim][$PF_6$]) with water in different ratios mediated the catalytic systems. In pure water, the yield of 1,2-diphenylacetylene was detected to be 72% (Table 2), whereas, in only ionic liquids, there was a dramatic decrease in the percentage of,2-diphenylacetylene, to be 58, 52, 48 and 70% in [bmim][$Tf_2N$], [emim][$Tf_2N$], [omim][$Tf_2N$] and [bmim][$PF_6$], respectively. With increase in the amount of water in the reaction media (as 1 : 3 and 1: 1) to the ionic liquid, there was an obvious rising in the yield of the favoured product (Table 4). These results are agreed with the previously reported impact of the ionic liquid in presence of water [42,43]. The mixed [bmim][$PF_6$]-water (1: 1) mediated the catalytic process with the highest yield of 1,2-diphenyethyne (entry 12, 87%, Table 4, TON and TOF values). The catalytic system was more progressed in the phosphorylated ionic liquid, as noted elsewhere [40,44].

Intriguingly, the mixed ionic liquid-water could strongly improve the solubility of the catalyst and the substrates, and so their miscibility, compared to the classical organic solvents [45]. The enhancement of both solubility and miscibility of the catalytic components could easily generate active catalytic species and/or form highly stable intermediates or transition-states [46].

Moreover, the easily extraction of the final product from the reaction media in the ionic liquids forced to measure the reusability of the desired Cu(II)-catalyst for several runs [47,48]. The reusing of $Cu_2L$ catalyst for Sonogashira protocol of phenylacetylene and bromobenzene in 10 mL of [bmim][$PF_6$]: $H_2O$ (1: 1) mixture at 80 °C for 20 h, was studied. The maximum recyclability of $Cu_2L$ was 5 runs awarding 87-85% of biaryl products. After 5 times of $Cu_2L$ reusing, the catalytic performance was slightly reduced and afforded 80% of the desired product.

It is worth to report here that the catalytic reaction could be achieved with better yield using iodobenzene more than with bromobenzene in the same applicable conditions (entries 1 and 2, Table 5) [39]. The oxidative addition step with iodobenzene is faster than that with bromobenzene in the catalytic cycles [49], due to the simultaneous C–I bond breaking than that C–Br than C–Cl in the aryl halide (see the mechanistic pathway in the oxidative addition step). The coupling yield of phenylacetylene with bromobenzene was influenced by the substituent on the bromobenzene affording various yields (entries 3–6, Table 5). The yield was reduced for the bromobenzene containing electron-donating group (methyl group) at *ortho*- and *para*-position (entries 3 and 4, 84% and 87%, respectively). On the other hand, bromobenzene containing more electron-withdrawing substituents (nitro groups) at *para*-position with only one exception of the more electron-donating group (methoxy group) exhibited excellent yield values (entries 5 and 6 with yielding 95 and 91%, respectively). The noteworthy electronic effect of the tolerated various functional groups on bromobenzene could be the main reason to control the reactivity of bromobenzene towards such coupling reactions with phenylacetylene [6,9,11]. The electron-withdrawing substituents on bromobenzene could encourage the C–Br braking in the oxidative addition step and so enhanced the catalytic reactivity of bromobenzene towards cross-coupling, whereas, electron-donating group of bromobenzene could push the electron density towards the C–Br bonding and so strengthens that bond and reduces the bromobenzene potential for C–C couplings.

In pursuit of new cross-coupling reactions, the reaction of phenylacetylene with some heterocyclic halides, *i.e.* 2-bromofuran and 2-bromothiophene, to give 2-(phenylethynyl)furan and 2-(phenylethynyl)thiophene, respectively, was probed under the best reaction conditions (Table 5, entries 7 and 8, respectively). The products, which characterized by NMR and mass spectra, afforded good yields (82 and 71%, respectively, as shown in Figs. S8 and S9, supplementary materials). 2-(Phenylethynyl)thiophene was already synthesized elsewhere by Domyati et *al.* [11] with yield 65% under harsh conditions of 135–140 °C in presence $K_2CO_3$ under aerobic conditions in DMF after 48 h catalyzed by Cu(I)–*N*-heterocyclic carbenes. The current Cu(II)-complex catalyst ($Cu_2L$) seems to be reactive with less consumed time and reaction temperature.

The novel Sonogashira cross-coupling reactions could be reported here, is the comparative yield percentages of the chemoselective product of the reaction of phenylacetylene with bromocyclopropane, as a representative example of alicyclic substrate, and with 1-bromopropane, as an example of aliphatic halide. Liu et al. reported an attempt to prepare C–C coupling product for an aliphatic precursor using alkylacetylenes with *p*-nitrobromobenzene in water affording excellent yields [49]. The synthesis of the novel C–C products, (cyclopropylethynyl)benzene and pent-1-yn-1-ylbenzene, respectively, was carried out in the

**Table 5**
$Cu_2L$ catalyzed Sonogashira C–C coupling reaction of phenylacetylene and different aryl, alicyclic or aliphatic halide derivatives..

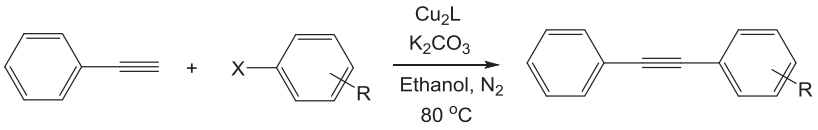


| Entry | —X | —R | Product | Yield (%)[b] |
|---|---|---|---|---|
| 1 | —I | H |  | 91 (88)[c] |
| 2 | —Br | H | 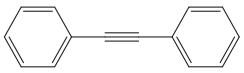 | 89 (86)[c] |
| 3 | —Br | *o*—Me | 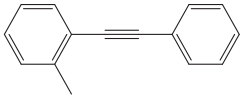 | 84 (79)[c] |
| 4 | —Br | *p*—Me | 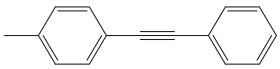 | 87 (84)[c] |
| 5 | —Br | *o*—$NO_2$ | 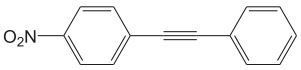 | 95 (88)[c] |
| 6 | —Br | *p*—OMe | 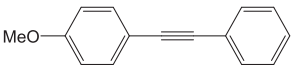 | 91 (87)[c] |
| 7 | 2-bromofuran | | 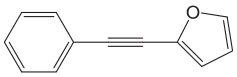 | 82 (75)[c] |
| 8 | 2-bromothiophene | | 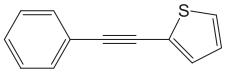 | 71 (67)[c] |
| 9 | bromocyclopropane | | 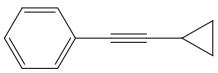 | 62 (58)[c] |
| 10 | 1-bromopropane | | 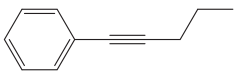 | 48 (46)[c] |

[a] Phenylacetylene (1.2 mmol), halobenzene (1.0 mmol), base ($K_2CO_3$, 3.0 mmol), and $Cu_2L$ as a catalyst (0.02 mmol) for 20 h.
[b] The yield percentages of the C–C product analyzed by GC-MS.
[c] Total isolated product which characterized by NMR spectra.

optimized reaction conditions of the catalyst ($Cu_2L$). The yield amounts were recorded in Table 5 (entries 9 and 10), for bromocyclopropane and 1-bromopropane, respectively, as assigned by GC-MS analyses (in the supplementary materials, Figs. 8 and 9). The yield values of the cross-coupling products are 62 and 48%, respectively. It is obvious that the C–C cross-coupling of the cyclic substrates afforded good chemical reactivity more than of the aliphatic ones [11,37]. $Cu_2L$ shows effective catalytic character towards aliphatic halides, although, Lima & Antunes [11] presented no formed C–C products of aliphatic halides with their Cu-free palladium salts with various phosphine ligands, as internal catalysts.

From Table 2 (entries 1 and 15), the comparison between the catalytic processes in absence (dry conditions) and presence of air oxygen could help to understand the role of air oxygen on the reactivity of the Cu-catalyst. The difference in the yield percentages (89% under $N_2$ atmosphere and 32% in air oxygen) could refer to the deactivation of the Cu-catalyst in air oxygen by Cu-oxygenation, which resulted probably from the formation of bridged oxy-, hydroxyl-, peroxy-dicopper [50] or superoxy-copper [51] complex, as

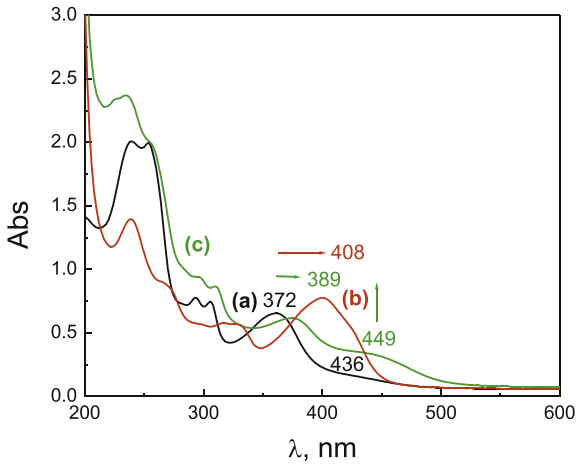


**Fig. 3.** UV/Vis. spectral scans of Cu-complex catalyst ($Cu_2L$) in ethanol at various conditions. (a) $Cu_2L$ in ethanol at room temperature; (b) $Cu_2L$ in ethanol after heating for 20 h at 80 °C in $N_2$ atmosphere; (c) $Cu_2L$ in the end of the catalytic process of C–C cross coupling in ethanol after 20 h at 80 °C in $N_2$ atmosphere.

less active catalyst.

The degree of the coordinated ligand stability as ligand effect, *i.e.* $H_4L$, could be estimated in the catalytic processes by repeating the C—C cross-coupling reaction in the typical conditions catalyzed by copper acetate instead of the current Cu-catalyst ($Cu_2L$). $Cu_2L$ afforded 89% of the chemoselective product, whereas, copper acetate gave 94% (entries 1 and 16, respectively). It is clear that $Cu_2L$ is highly stable due to the fairly stability of its coordinated ligand compared to copper acetate and this could be noted on its reactivity as a homogeneous catalyst for Sonogashira coupling protocol through the formation of active catalyst intermediate (see the mechanism, Scheme 2). Indeed, the ligand could have a notable effect of the catalytic reactivity and so the coupling reaction could probably depending on the type of coordinated donor atoms (N and/or O-donor), as recorded before by Bolm et al. [52]. That consideration was also observed by other Cu(II)-species using various structural ligands because the coupling reaction conditions were differentiated by Cu(II)-catalyst to another depending on the ligand nature [11,14,29]. The increases in the yield percentages could be related to the excess amount of copper acetate in the reaction media, which probably acted as a homogeneous catalyst.

### 3.3. Proposed mechanism

Ethanol is the best solvent for the Sonogashira coupling protocol, this could be predestined by a simple test through monitoring of the UV—Vis. spectrophotometric changes of $Cu_2L$ (Fig. 3a) in ethanol at room temperature under dry conditions (Fig. 3b) and in ethanol after 20 h at 80 °C under dry conditions (Fig. 3c) (0.02 mmol of $Cu_2L$ in 10 mL ethanol). From both spectral scans (Figs. 3b,c), there were strong observable shifts of the characteristic ML-CT band (372 nm) to be at 408 nm after heating, and also the *d—d* band was shifted and became broader band (from 436 nm to 481 nm). Moreover, with GC analysis of the products in that test, acetaldehyde was detected in very trace amounts. It could be concluded that ethanol could act as reducing agent for the formation of the active Cu(0)-complex catalyst and could enhance the catalytic reactivity of $Cu_2L$ compared to other applicable solvents.

Despite, the mechanism of the Sonogashira cross-coupling reaction is still not enough studied and not so clear [45], a plausible mechanistic pathway was suggested in Scheme 2. The mechanism started with formation of the active species of Cu(0)-catalyst (**1**), as reported for the Cu-free Pd-catalysts [52—55]. The transient Cu-acetylide was formed in the catalytic reaction, as detected previously [52], which due to the reaction if the Cu(II)-precursor with phenylacetylene. The transformation of the initial Cu(II) complex, as a pre-catalyst, to the active Cu(0)-species could be taken place by the influence of the solvent (*i.e.* ethanol within the alcoholic group, as detected previously by Hajipour et *al.* for the reduction of silica gel supported Fe(III) complex to Fe(I)-species as a heterogeneous catalyst in various Sonogashira reactions [56]). The alcoholic group of ethanol, with reducing character, could increase the reactivity of $Cu_2L$ catalyst to be reduced to Cu(0)-one, as investigated here. Moreover, phenylacetylene and the base could assist in the reduction of $Cu_2L$ to **1** [56]. Oxidative addition of Cu(0)-species could be carried out by halobenzene [53] (as electrophilic organic species with electron-withdrawing group) [57] to form active Cu(II)-species (**2**) by adding halobenzene to the coordination sphere of Cu(II) ion. Halobenzene, as electron-rich aryl halides, demands harsh conditions in the cross-coupling reactions, *i.e.* long time at high temperature, which could diminish the catalytic potential of $Cu_2L$ towards oxidative addition with bond break of Ar—X and bonding to Cu(II) ion [37]. Oxidation of Cu(0)-complex (**1**) could be progressed due to its ability to donate electrons through the formation of new Cu—C bond with aryl halides but could need drastic reaction conditions [37]. This explains why most of the Sonogashira cross-coupling reactions requires long time and high reaction temperature. Furthermore, $K_2CO_3$, as a base, speeds also the oxidative addition step [58]. Ar—X with electron-withdrawing/donating group features could be touched here by the alternative amount of the yield percentages of the target product depending on the attached electron-withdrawing or donating group of Ar—moiety. The more electron-donating group of Ar—X, *e.g.* bromocyclopropane and 1-bromopropane afforded moderate to low yields (62 and 48%, respectively, Table 5), whereas, the more electron-withdrawing group, *e.g.* 2-nitro-1-bromobenzene, gave excellent yield (95%, Table 5). Consequently, Ar—X with electron-withdrawing group could speed the formation of intermediate **3** and could also improve the yields of the C—C products. Those obtains were due to that the more electron-withdrawing group facilitates the Ar—X bond-breaking more than that of the more electron-donating group.

The role of the base could be observed in the extraction of the halide ion with replacement of carbonate anion affording Cu(II)-acyl species (**3**). Intermediate **3** was attacked by phenylacetylene to form Cu(II)-biphenyl intermediate complex (**4**) within transmetalation [54]. To understand the transmetallation step with attack of phenylacetylene to the central metal ion, Cu(II) ion, previously, it was recognized that the presence of primary or secondary amines could activate phenylacetylene within its deprotonation [59]. Therefore, in the absence of amines here, the phenylacetylene deprotonation could take place on Cu(II) ion through its coordination to Cu(II) ion in the intermediate **3** to give **4** and could be accelerated by $K_2CO_3$, pushing the electron density away from phenylacetylene [60]. Reductive elimination produced the final product with generating the active Cu(0)-catalyst (**1**), which could be achieved in the presence of nucleophilic organic species [55] for another catalytic cycle (Scheme 2).

The transformation of $Cu_2L$ through the catalytic process to Cu(II)/Cu(0)-species could be revealed by spectrophotometric scans of $Cu_2L$ before and after completion of the catalytic process, as presented in Fig. 3a—c. The notable shift of the ML-CT band in $Cu_2L$ before inserting into the catalytic reaction was located at 372 nm and at the end of the catalytic process was found at 389 nm. Also, the remarked shift of the *d—d* transition band from 436 to 449 nm could prove the transformation of $Cu_2L$ to the generated of Cu(II)/C(0)-intermediates in the catalytic cycles [11].

### 3.4. DFT calculations

The optimal molecular structures, HOMOs, and LUMOs maps of $H_4L$ and $Cu_2L$ molecules are shown in Fig. S14 and Fig. 4, respectively. The calculated data of DFT are reported in Table 6. The potential interaction of $H_4L$ and $Cu_2L$ could be estimated by HOMO and LUMO. HOMO refers to the electron density donating capability [61] and LUMO is associated with electron density accepting experience [25,26]. Both, high energy values of HOMO ($E_{HOMO}$) and low energy values ($E_{LUMO}$) are interrelated with the strong metal-coordinating binding of $H_4L$ towards $Cu^{2+}$ ions [62]. The difference between the $E_{HOMO}$ and $E_{LUMO}$ values epitomizes the values of energy gap (ΔE). Hence, $Cu_2L$ as homogeneous cross-coupling catalyst awarded a higher value of energy gap (ΔE) in both gas and water phases. This could be related to high catalytic potential of $Cu_2L$ towards C—C cross-coupling reactions, specifically towards (oxidative addition and reductive elimination steps) [63].

From the distribution of the frontier molecule orbital density, the electron density of the HOMO in $H_4L$ is predominantly located in the benzoyl hydrazone and sulfonate moieties. The electron density of the LUMO is mostly positioned on the entire molecule except the polar sodium sulfonate group. A similar partial change of

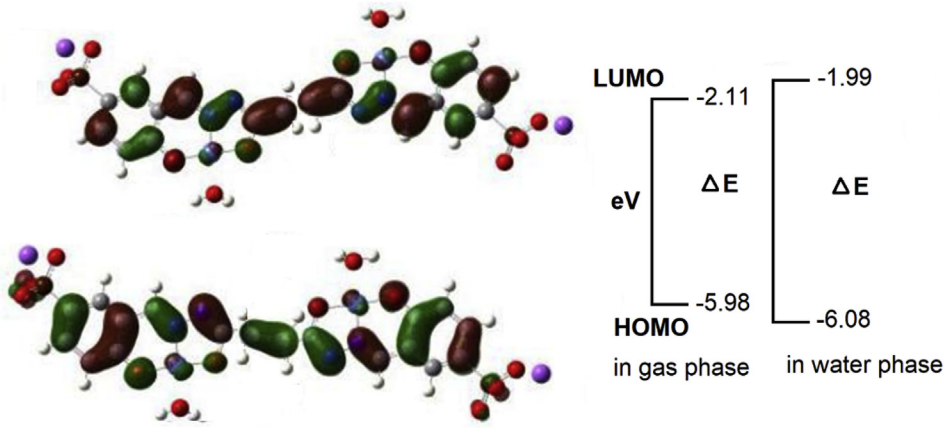


**Fig. 4.** Frontier molecular orbital (HOMOs and LUMOs) of Cu-complex ($Cu_2L$).

**Table 6**
Quantum data for $H_4L$ and $Cu_2L$ molecules in gas and water phases.

| Compound | $H_4L$ | | $Cu_2L$ | |
|---|---|---|---|---|
| | gas | water | gas | water |
| $E_{HOMO}$ (eV) | −5.73 | −5.81 | −5.98 | −6.08 |
| $E_{LUMO}$ (eV) | −2.10 | −2.03 | −2.11 | −1.99 |
| ΔE (eV) | 3.63 | 3.78 | 3.87 | 4.09 |
| χ (eV) | 3.91 | 3.92 | 4.05 | 4.04 |
| η (eV) | 1.01 | 1.89 | 1.93 | 2.04 |
| σ ($eV^{-1}$) | 0.99 | 0.52 | 0.51 | 0.49 |
| ω (eV) | 7.56 | 4.06 | 4.25 | 4.04 |

the electron density distribution was exposed of the HOMOs and LUMOs for $Cu_2L$ molecule with expectation for an electron transfer from HOMO to the LUMO forming a bond between the reagents in the C—C cross-coupling mechanism (oxidative addition and reductive elimination), as an effective catalyst [64].

The computed value of global electronegativities of $H_4L$ and $Cu_2L$ was determined. The molecule that the low value of χ associated with the strong donating ability of electron density. This is why $H_4L$ has lower value of χ in gas and water phases, which could react as reducing ligand and, hence, could be contributed for coordination to $Cu^{2+}$ ion with forcing for formation of the reduced active catalyst complex in the catalytic cross-coupling. Therefore, $Cu_2L$ has less electron density, which enhances its reactivity as a catalyst towards Sonogashira cross-couplings. This could probably force $Cu_2L$ to form an active reduced catalyst intermediate in the catalytic cycle (Cu(I)/Cu(0)-species, Scheme 2) [65].

The hardness (η), as an indicator values for the stability of the formed compounds, and softness (σ) values [66] were also determined. Softness values (σ) are measurements for the molecules' polarizabilities. The more soft molecules could have high reactivity towards catalytic protocols [54]. From Table 6, $Cu_2L$ has high values of η with the low values of σ, compared to $H_4L$. The better applicable complex species as homogeneous catalysts are those with high dipole moment [63]. Here, $Cu_2L$ has dipole moment with appreciable polarity, which progresses its catalytic efficiency towards Sonogashira cross-coupling protocols.

## 4. Conclusions

The high coordination ability of the new polydentate ligand ($H_4L$), *bis*(5-sodium sulfonate-2-hydroxybenzylidene)succinylhydrazone towards copper (II) ions, provided a novel Cu(II)-complex, $Cu_2L$, which was characterized by alternative physico-chemical tools. $Cu_2L$ showed excellent catalytic affectivity as a homogeneous catalyst in Sonogashira cross-coupling protocol of phenylacetylene with bromobenzene in ethanol at 80 °C for 20 h. Lower catalytic reactivity was observed by using other polar solvents, *i.e.* water, water-ethanol mixtures, THF, DMF, DMSO and under free solvent conditions. The catalytic efficiency of $Cu_2L$ was improved in ionic liquids—aqueous media (1 : 1, binary mixture) provided excellent yield percentages of the desired product (1,2-diphenyethyne). Hence, the recycling of the Cu-catalyst was successfully attempted five times. A mechanistic pathway has been proposed for Sonogashira cross coupling reactions based on the oxidative addition and reductive eliminations steps. DFT studies calculated the electronic configurations energy of HOMO and LUMO orbitals, energy gap between orbitals (ΔE), electronegativity, hardness and softness for $H_4L$ and $Cu_2L$. All data of the theoretical calculations refer to an agreement with the experimental obtains of the catalytic potential of $Cu_2L$.

## Appendix A. Supplementary data

Supplementary data to this article can be found online at https://doi.org/10.1016/j.jorganchem.2019.120985.

## References

[1] (a) C.M. So, F.Y. Kwong, Chem. Soc. Rev. 40 (2011) 4963–4972;
(b) R. Chinchilla, C. Najera, Chem. Rev. 107 (2007) 874–922.
[2] D. Wang, D. Denux, J. Ruiz, D. Astruc, Adv. Synth. Catal. 355 (2013) 129–142.
[3] C.C.J. Seechurn, M.O. Kitching, T.J. Colacot, V. Snieckus, Angew. Chem. Int. Ed. 51 (2012) 5062–5085.
[4] B. Agrahari, S. Layek, Anuradha, R. Ganguly, D.D. Pathak, Inorg. Chim. Acta 471 (2018) 345–354.
[5] N. Touj, S. Yasar, N. Ozdemir, N. Hamdi, I. Ozdemir, J. Organomet. Chem. 860 (2018) 59–71.
[6] A.R. Hajipour, S.M. Hosseini, F. Mohammadsaleh, New J. Chem. 40 (2016) 6939–6945.
[7] A.R. Hajipour, F. Mohammadsaleh, Tetrahedron Lett. 55 (2014) 3459–3462.
[8] (a) B. Ghanbari, L. Shahhoseini, H. Hosseini, M. Bagherzadeh, A. Owczarzak, M. Kubicki, J. Organomet. Chem. 866 (2018) 72–78;
(b) T. Mino, S. Suzuki, K. Hirai, M. Sakamoto, T. Fujita, Synlett 9 (2011) 1277–1280.
[9] (a) S.S. Devkule, M.S. More, S.S. Chavan, Inorg. Chim. Acta 455 (2017) 183–189;
(b) W. Xu, B. Yu, H. Sun, G. Zhang, W. Zhang, Z. Gao, Appl. Organomet. Chem. 29 (2015) 301–304.
[10] (a) A.A. Liori, I.K. Stamatopoulos, A.T. Papastavrou, A. Pinaka, G.C. Vougioukalakis, Eur. J. Org. Chem. 44 (2018) 6134–6139;
(b) A.Y. Mitrofanov, A.V. Murashkina, I. Martín-García, F. Alonso, I.P. Beletskaya, Catal. Sci. Technol. 7 (2017) 4401–4412.
[11] (a) D. Domyati, R. Latifi, L. Tahsini, J. Organomet. Chem. 860 (2018) 98–105;
(b) P.G. de Lima, O.A.C. Antunes, Tetrahedron Lett. 49 (2008) 2506–2509.
[12] A.Y. Mitrofanov, A.G. Bessmertnykh-Lemeune, I.P. Beletskaya, Inorg. Chim.

Acta 431 (2015) 297–301.
[13] M. Trivedi, G. Singh, A. Kumar, N.P. Rath, Dalton Trans. 43 (2014) 13620–13629.
[14] D.P. Singh, D.S. Raghuvanshi, K.N. Singh, V.P. Singh, J. Mol. Catal. A 379 (2013) 21–29.
[15] (a) V. Niel, V.A. Milway, L.N. Dawe, H. Grove, S.S. Tandon, T.S.M. Abedin, T.L. Kelly, E.C. Spencer, J.A.K. Howard, J.L. Collins, D.O. Miller, L.K. Thompson, Inorg. Chem. 47 (2008) 176–189;
(b) A.-M. Stadler, J. Harrowfield, Inorg. Chim. Acta 362 (2009) 4298–4314.
[16] A. Kumar, R. Borthakur, A. Koch, O.B. Chanu, S. Choudhury, A. Lemtur, R.A. Lal, J. Mol. Struct. 999 (2011) 89–97.
[17] V.P. Singh, S. Singh, J. Coord. Chem. 64 (2011) 3068–3080.
[18] G.G. Mohamed, M.M. Omar, A.M.M. Hindy, Spectrochim. Acta A 6 (2005) 1140–1150.
[19] M.S.S. Adam, Monatshefte Chem. 146 (2015) 1823–1836.
[20] X. Liu, J.-R. Hamon, Coord. Chem. Rev. 389 (2019) 94–118.
[21] S. Shylesh, V. Schunemann, W.R. Thiel, Angew. Chem., Int. Ed. 49 (2010) 3428–3459.
[22] K. Sonogashira, in: B.M. Trost, I. Fleming (Eds.), Comprehensive Organic Synthesis, vol. 3, Pergamon, New York, 1991.
[23] M.S.S. Adam, A.D. Mohamad, O.M. El-Hady, Monatshefte Chem. 145 (2014) 435–445.
[24] M.J. Frisch, G.W. Trucks, H.B. Schlegel, G.E. Scuseria, M.A. Robb, J.R. Cheeseman, G. Scalmani, V. Barone, B. Mennucci, G.A. Petersson, H. Nakatsuji, M. Caricato, X. Li, H.P. Hratchian, A.F. Izmaylov, J. Bloino, G. Zheng, J.L. Sonnenberg, M. Hada, M. Ehara, K. Toyota, R. Fukuda, J. Hasegawa, M. Ishid, T. Nakajima, Y. Honda, O. Kitao, H. Nakai, T. Vreven, J.A. Montgomery, J.E. Peralta, F. Ogliaro, M. Bearpark, J.J. Heyd, E. Brothers, K.N. Kudin, V.N. Staroverov, T. Keith, R. Kobayashi, J. Normand, K. Raghavachari, A. Rendell, J.C. Burant, S.S. Iyengar, J. Tomasi, M. Cossi, N. Rega, J.M. Millam, M. Klene, J.E. Knox, J.B. Cross, V. Bakken, C. Adamo, J. Jaramillo, R. Gomperts, R.E. Stratmann, O. Yazyev, A.J. Austin, R. Cammi, C. Pomelli, J.W. Ochterski, R.L. Martin, K. Morokuma, V.G. Zakr-Zewski, G.A. Voth, P. Salvador, J.J. Dannenberg, S. Dapprich, A.D. Daniels, O. Farkas, J.B. Foresman, J.V. Ortiz, J. Cioslowski, D.J. Fox, Gaussian, Inc., Wallingford CT, 2010.
[25] H.M. Abd El-Lateef, M.S.S. Adam, M.M. Khalaf, J. Taiwan Inst. Chem. Eng. 88 (2018) 286–304.
[26] L.H. Abdel-Rahman, A.M. Abu-Dief, M.S.S. Adam, S.K. Hamdan, Catal. Lett. 146 (2016) 1373–1396.
[27] U. Golla, A. Adhikary, A.K. Mondal, R.S. Tomar, S. Konar, Dalton Trans. 45 (2016) 11849–11863.
[28] R. Borthakur, A. Kumar, R.A. Lal, Spectrochim. Acta a 149 (2015) 621–629.
[29] R. Borthakur, A. Kumar, A. Lemtur, R.A. Lal, RSC Adv 3 (2013) 15139–15147.
[30] S.D. Kurbah, A. Kumar, I. Syiemlieh, M. Asthana, R.A. Lal, Inorg. Chem. Commun. 86 (2017) 39–43.
[31] S.D. Kurbah, A. Kumar, I. Syiemlieh, R.A. Lal, Polyhedron 139 (2018) 80–88.
[32] S.D. Kurbah, A. Kumar, O.S. Ozukum, I. Syiemlieh, Ram A. Lal, J. Coord. Chem. 70 (2017) 2969–2985.
[33] M.F. Iskander, L. El-Sayed, N.M.H. Salem, R. Werner, W. Haase, J. Coord. Chem. 58 (2005) 125–139.
[34] (a) M.S.S. Adam, e4234, Appl. Organomet. Chem. 32 (2018);
(b) M.S.S. Adam, M.A. Al-Omair, F. Ullah, Res. Chem. Intermed. 45 (2019) 4653–4675.
[35] M. Enamullah, M.A. Quddus, M.M. Rahman, T.E. Burrow, J. Mol. Struct. 1130 (2017) 765–774.
[36] M. Bagherzadeh, N. Mousavi, M. Zare, S. Jamali, A. Ellern, L.K. Woo, Inorg. Chim. Acta 451 (2016) 227–232.
[37] K. Karami, S. Abedanzadeh, P. Herves, RSC Adv 6 (2016) 93660–93672.
[38] N. Liu, C. Liu, Q. Xu, Z. Jin, Eur. J. Org. Chem. 23 (2011) 4422–4428.
[39] S. Asha, A.M. Thomas, S.M. Ujwaldev, G. Anilkumar, ChemistrySelect 1 (2016) 3938–3941.
[40] N. Iranpoor, H. Firouzabadi, Y. Ahmadi, Eur. J. Org. Chem. 2 (2012) 305–311.
[41] J. Li, S. Yang, W. Wu, H. Jiang, Eur. J. Org. Chem. 11 (2018) 1284–1306.
[42] M. Wang, X. Yuan, H. Li, L. Ren, Z. Sun, Y. Hou, W. Chu, Catal. Commun. 58 (2015) 154–157.
[43] R. Wang, B. Twamley, J.B. Shreeve, J. Org. Chem. 71 (2006) 426–429.
[44] J. Zhang, M. Đakovic, Z. Popovic, H. Wu, Y. Liu, Catal. Commun. 17 (2012) 160–163.
[45] (a) A. Corma, H. Garcia, A. Leyva, Tetrahedron 61 (2005) 9848–9854;
(b) S.A. Timofeeva, M.A. Kinzhalov, E.A. Valishina, K.V. Luzyanin, V.P. Boyarskiy, T.M. Buslaeva, M. Haukka, V.Yu. Kukushkin, J. Catal. 329 (2015) 449–456.
[46] P. Mastrorilli, A. Monopoli, M.M. Dell'Anna, M. Latronico, P. Cotugno, A. Nacci, Top. Organomet. Chem. 51 (2015) 237–285.
[47] T. Fukuyama, M.T. Rahman, S. Maetani, I. Ryu, Chem. Lett. 40 (2011) 1027–1029.
[48] J.R. Harjani, T.J. Abraham, A.T. Gomez, M.T. Garcia, R.D. Singer, P.J. Scammells, Green Chem. 12 (2010) 650–655.
[49] (a) M. Ghabdian, M.A. Nasseri, A. Allahresani, A. Motavallizadehkakhky, Appl. Organomet. Chem. 32 (2018) e4545;
(b) N. Liu, C. Liu, Q. Xu, Z. Jin, Eur. J. Org. Chem. 23 (2011) 4422–4428.
[50] H.V. Obias, Y. Lin, N.N. Murthy, E. Pidcock, E.I. Solomon, M. Ralle, N.J. Blackburn, Y.-M. Neuhold, A.D. Zuberbühler, K.D. Karlin, J. Am. Chem. Soc. 120 (49) (1998) 12960–12961.
[51] D.J.E. Spencer, N.W. Aboelella, A.M. Reynolds, P.L. Holland, W.B. Tolman, J. Am. Chem. Soc. 124 (2002) 2108–2109.
[52] (a) J.-B. Peng, F.-P. Wu, C.-L. Li, X. Qia, X.-F. Wu, Eur. J. Org. Chem. 11 (2017) 1434–1437;
(b) E. Zuidema, C. Bolm, Chem. Eur. J. 16 (2010) 4181–4185;
(c) L.-H. Zou, A.J. Johansson, E. Zuidema, C. Bolm, Chem. Eur J. 19 (2013) 8144–8152.
[53] X. Qi, H.-J. Ai, C.-X. Cai, J.-B. Peng, F. Zheng, X.-F. Wu, Eur. J. Org. Chem. (2017) 2940–2943.
[54] A.M. Mak, Y.H. Lim, H. Jong, Y. Yang, C.W. Johannes, E.G. Robins, M.B. Sullivan, Organometallics 35 (2016) 1036–1045.
[55] S.E. Denmark, M.G. Edwards, J. Org. Chem. 71 (2006) 7293–7306.
[56] A.R. Hajipour, P. Abolfathi, Z. Tavangar-Rizi, e4353, Appl. Organomet. Chem. 32 (2018).
[57] K. Sonogashira, E. Negishi, A. de Meijere, Handbook of Organopalladium Chemistry for Organic Synthesis, Wiley-Interscience, New York, 2002.
[58] S. Fujimori, T.F. Knopfel, P. Zarotti, T. Ichikawa, D. Boyall, E.M. Carreira, Bull. Chem. Soc. Jpn. 80 (2007) 1635–1657.
[59] T. Ljungdahl, T. Bennur, A. Dallas, H. Emtenas, J. Martensson, Organometallics 27 (2008) 2490–2498.
[60] A. Soheili, J. Albaneze-Walker, J.A. Murry, P.G. Dormer, D.L. Hughes, Org. Lett. 5 (2003) 4191–4194.
[61] K. Fukui, Theory of Orientation and Stereoselection, Springer-Verlag, New York, 1975.
[62] J. Haque, V. Srivastava, C. Verma, H. Lgaz, R. Salghi, M. Quraishi, New J. Chem. 41 (2017) 13647–13662.
[63] M.S.S. Adam, H.M. Abd El-Lateef, K.A. Soliman, J. Mol. Liq. 250 (2018) 307–322.
[64] J.S.M. Anderson, J. Melin, P.W. Ayers, J. Chem. Theory Comput. 3 (2007) 358–374.
[65] T. Wang, M. Wang, S. Fang, J.-Y. Liu, Organometallics 33 (2014) 3941–3949.
[66] R.G. Parr, P.K. Chattaraj, J. Am. Chem. Soc. 113 (1991) 1854–1855.